How to cite: *Angew. Chem. Int. Ed.* **2021**, *60*, 18209–18216
International Edition: doi.org/10.1002/anie.202105342
German Edition: doi.org/10.1002/ange.202105342

Supramolecular Polymers

Tricomponent Supramolecular Multiblock Copolymers with Tunable Composition via Sequential Seeded Growth

Aritra Sarkar, Ranjan Sasmal, Angshuman Das, Akhil Venugopal, Sarit S. Agasti, and Subi J. George**

Abstract: *Synthesis of supramolecular block co-polymers (BCP) with small monomers and predictive sequence requires elegant molecular design and synthetic strategies. Herein we report the unparalleled synthesis of tri-component supramolecular BCPs with tunable microstructure by a kinetically controlled sequential seeded supramolecular polymerization of fluorescent π-conjugated monomers. Core-substituted naphthalene diimide (cNDI) derivatives with different core substitutions and appended with β-sheet forming peptide side chains provide perfect monomer design with spectral complementarity, pathway complexity and minimal structural mismatch to synthesize and characterize the multi-component BCPs. The distinct fluorescent nature of various cNDI monomers aids the spectroscopic probing of the seeded growth process and the microscopic visualization of resultant supramolecular BCPs using Structured Illumination Microscopy (SIM). Kinetically controlled sequential seeded supramolecular polymerization presented here is reminiscent of the multistep synthesis of covalent BCPs via living chain polymerization. These findings provide a promising platform for constructing unique functional organic heterostructures for various optoelectronic and catalytic applications.*

Introduction

Controlled supramolecular polymerization of functional monomers has emerged recently as an attractive bottom-up synthetic strategy for the construction of precision organic materials with controlled structure and composition.[1] Detailed mechanistic insights into the supramolecular polymerization[2] and associated pathway complexity of the process,[3] expedited various synthetic designs such as living seeded supramolecular polymerization,[4,5] crystallization driven self-assembly[6] and bio-inspired reaction-driven supramolecular polymerization[7] as efficient strategies for the controlled synthesis of self-assembled materials with low-dispersity. The next level of structural control required would be the synthesis of multi-component supramolecular polymers with predictive sequence and microstructure for various applications.[8] In this context, supramolecular block-copolymerization of the complementary π-conjugated monomers can provide functional axial organic heterostructures with enhanced exciton migration efficiency along the π-stacking direction,[9] which are envisioned to have potential applications in optoelectronics and photo-catalysis.[10]

Crystallization-driven self-assembly (CDSA) of kinetically stable poly (ferrocenyldimethylsilane) (PFS)-core containing copolymers is one of the well-established synthetic strategies for functional supramolecular block copolymers (BCPs) with complex sequences, topology and functions.[6] However, unlike the well-established block copolymerization reactions in its covalent polymeric analogs,[11] and CDSA approach, supramolecular block copolymerization with π-conjugated small molecules directed by specific supramolecular interaction is synthetically challenging,[8] majorly due to the fast monomer exchange dynamics and lack of characterization techniques to probe the resultant microstructure. Thus, only recently limited but elegant synthetic attempts have been made to construct supramolecular BCPs of small monomers, which are known to exhibit monomer exchange dynamics. This includes thermodynamically controlled supramolecular co-polymerization of the monomers,[12] and sequential addition of monomers using kinetically controlled seed induced living supramolecular polymerization (LSP).[13,14]

However, despite these promising advances, supramolecular block co-polymerization for the synthesis of multicomponent heterostructures with more than two functional monomers and with tunable sequence still remains to be an important challenge to be addressed. Synthesis of tri-component BCPs are well-established in conventional covalent polymers using living chain polymerization by the sequential addition of monomers.[15] In a pioneering work towards this direction, Manners and co-workers have demonstrated the extension of CDSA strategy to three different dye-labeled poly-ferrocenyldimethylsilane crystallizable core to achieve tricomponent block copolymers with tunable sequence.[16] Although, seed-induced LSP offers the possibility of sequential addition of monomers during the supramolecular polymerization process, lack of appropriate monomer designs with structural similarity and independent probing features restricts the synthesis of similar complex microstructures in supramolecular copolymers of small dynamic monomers.[8b] Supramolecular block-copolymerization strategies reported till date have used monomers with minimal structural

[*] Dr. A. Sarkar, R. Sasmal, A. Das, A. Venugopal, Dr. S. S. Agasti, Prof. Dr. S. J. George
New Chemistry Unit (NCU) and School of Advanced Materials (SAMat), Jawaharlal Nehru Centre for Advanced Scientific Research (JNCASR)
Jakkur, Bangalore, 560064 (India)
E-mail: sagasti@jncasr.ac.in
george@jncasr.ac.in

Supporting information and the ORCID identification number(s) for the author(s) of this article can be found under: https://doi.org/10.1002/anie.202105342.

mismatch to avoid narcissistically self-sorted assemblies,[17] as delicate free-energy of interactions dictate the co-assembly of monomers.[13c] In this context, it has been shown independently by our group[12b,13a] and Würthner's group[13b,c] that core-substituted arylene dimiides[18] provide an ideal family of monomers to establish the concept of supramolecular block-polymerization and to construct functional nanostructures, as monomer's functional properties can be easily modulated by minimal structural change at their core-substitution. Moreover, the unique spectral properties of core-substituted arylenediimides provide an excellent tool for the spectroscopic and microscopic characterization of the resultant heterostructures. Thus, we have recently employed core-substituted NDIs[18a] for the synthesis of supramolecular BCPs under both thermodynamic[12b] and kinetic experimental conditions,[13a] which provide a linear hetero-junction topology for the cNDI assemblies, compared to the well-studied cNDI based orthogonal heterojunctions constructed by Matile and co-workers using self-organizing surface-initiated polymerization[19] or using a zipper approach[20] reaction on the surface.

In this manuscript, we have elevated the complexity of supramolecular BCP design, by reporting tri-component supramolecular BCPs with tunable microstructure, using a kinetically controlled, sequential seed-induced LSP process (Figure 1). Three amphiphilic core-disubstituted naphthalene diimide derivatives with ethoxy (**1**), ethane thiol (**2**) and isopropyl amine (**3**) core substitution, are used as the structurally similar monomers with distinct spectral properties. Further, the monomer design also involves a tripeptide sequence containing the diphenylalanine motif as a hydrogen-bonding motif in a nonpolar medium, to ensure a pathway complexity-driven, kinetically controlled cooperative supramolecular polymerization process, similar to the various protein aggregation process.[21,22] Detailed spectroscopic probing and visualization of the resultant BCPs using structured illumination microscopy (SIM)[23] showed the presence of multi-component axial heterostructures with fluorescent emissive blocky segments.

The triblock supramolecular BCPs synthesized by Manners group[16] contain the blocky domains of the red, green and blue dyes at the peripheral corona of the stacked polymers and thus provides an interesting material for light-harvesting and as fluorescent barcodes.[16] In contrast to this unique example, the multiblock fluorescent BCPs presented here, have the π-stacked fluorophores at the backbone of the assemblies. This molecular organization is preferred for an excitonic migration and energy transport along the stacks which can be tapped further for photocatalysis and various other applications in supramolecular electronics. Thus, these supramolecular BCPs can be called as organic heterostructures, which are reminiscent of the inorganic heterostructures.

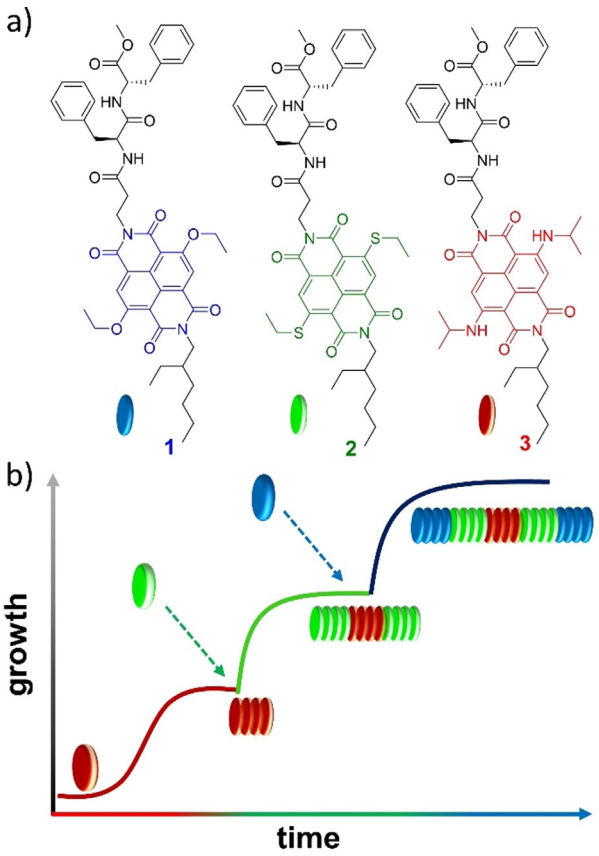

Figure 1. a) Molecular structures of the monomers **1**, **2** and **3** used for the synthesis of tricomponent supramolecular block co-polymers. b) Schematic illustration of sequential seeded supramolecular polymerization process for the synthesis of tricomponent BCP with a particular microstructure.

Results and Discussion

Supramolecular Homopolymerization of Monomers 1, 2, and 3

Monomers **1, 2**, and **3** were synthesized by multi-step synthetic procedures (Scheme S1–S6) and are well-characterized by ^{1}H, ^{13}C NMR spectroscopy, and mass spectrometry. Supramolecular homopolymerization of monomers **1**–**3** could be induced in TCE/methylcyclohexane (MCH) solvent mixture of varying composition (TCE/MCH, 10/90 (v/v) to TCE/MCH, 5/95 (v/v) for **1**, TCE/MCH, 15/85 (v/v) to TCE/MCH, 5/95 (v/v) for **2**, TCE/MCH, 10/90 (v/v) to TCE/MCH, 5/95 (v/v) for **3**) and was probed spectroscopically (Figure S1–S4). Molecules **1**, **2**, and **3** forms emissive assemblies which are evident from fluorescent and lifetime measurements in their self-assembled state (Figure S1c, S2c, S3c, and S4). Emissive nature of the organized monomers in the resultant supramolecular homopolymers (Figure 2 a) facilitated their visualization using structured illumination microscopy (SIM), which revealed the formation of one-dimensional fibrous assemblies, depicted as blue ($\lambda_{max} = 510$ nm), green ($\lambda_{max} = 567$ nm), and red-fluorescent ($\lambda_{max} = 639$ nm) assemblies of **1**, **2** and **3**, respectively (Figure 2 b–d). The distinct absorption and emission profiles of stacked monomers **1**–**3** (Figure 2 a) would aid the independent spectroscopic probing of monomers during the multicomponent supramolecular co-polymerization process and the orthogonal visualization of the resultant supramolecular copolymers using SIM microscopy (vide infra). Independent SIM imaging showed that monomer **1** gets exclusively excited at Channel I ($\lambda_{ex} = 488$ nm, $\lambda_{coll} =$

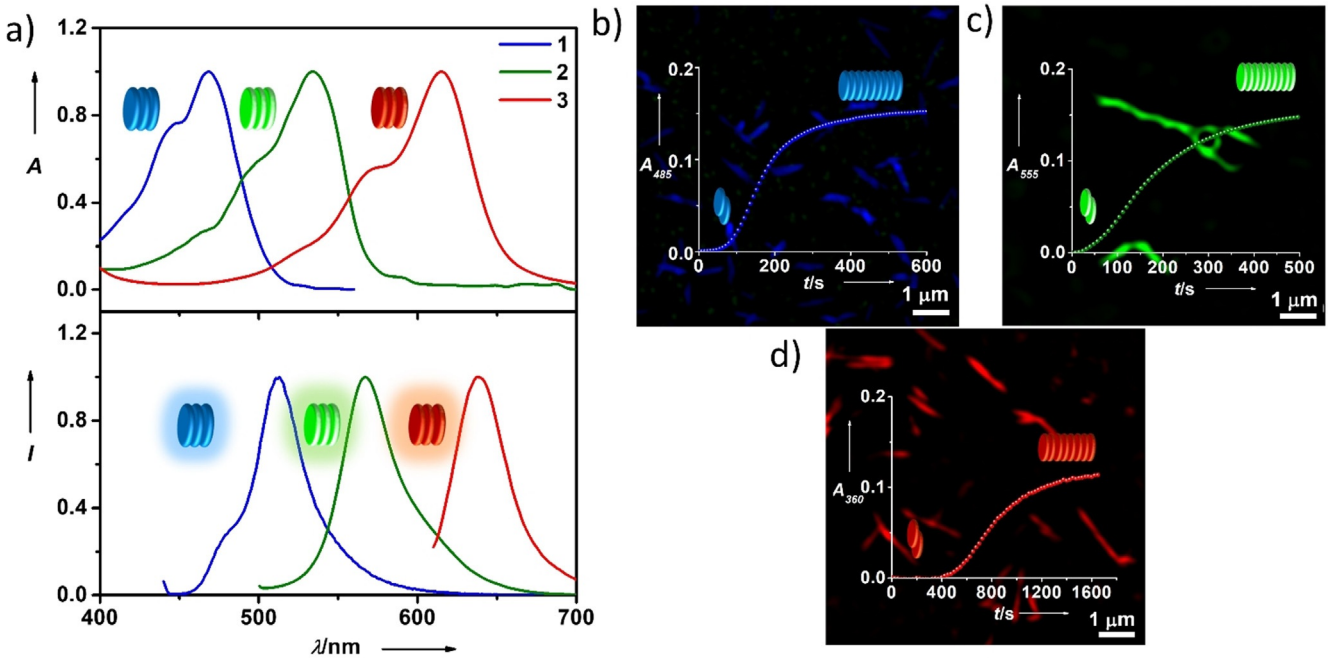

Figure 2. a) Normalized absorption and emission spectra of supramolecular homopolymers of **1** (blue), **2** (green) and **3** (red) with distinct absorption and emission profiles ([**1**] = [**2**] = [**3**] = 1.5×10^{-5} M, TCE/MCH, 10/90 (v/v)). The emission spectra of monomer **1** (λ_{ex} = 430 nm), **2** (λ_{ex} = 530 nm) and **3** (λ_{ex} = 600 nm). b) Time dependent absorbance changes (monitored at 475 nm for **1**, 555 nm for **2** and 360 nm for **3**) of b) **1**, c) **2** and d) **3**, which exhibits kinetically controlled cooperative supramolecular polymerization of the monomers. In the background of figures b–d, it shows the SIM images (inset) of the corresponding assemblies imaged through Channel I, Channel II, and Channel III, respectively which shows the presence of blue, green and red emitting supramolecular polymers ([**1**] = [**2**] = [**3**] = 1.5×10^{-5} M, TCE/MCH, 10/90 (v/v), Channel I: λ_{ex} = 488 nm, λ_{coll} = 495–575; Channel II: λ_{ex} = 561 nm, λ_{coll} = 570–650, Chanel III: λ_{ex} = 642 nm, λ_{coll} = 655–800 nm.

495–575), monomer **2** gets excited at Channel I (λ_{ex} = 488 nm, λ_{coll} = 495–575) and Channel II (λ_{ex} = 561 nm, λ_{coll} = 570–650), and monomer **3** gets excited at Channel II (λ_{ex} = 561 nm, λ_{coll} = 570–650), and Channel III (λ_{ex} = 642 nm, λ_{coll} = 655–800 nm), which would facilitate the visualization of supramolecular co-polymers with different sequences (Figure S5–S8).

Pathway Complexity of Monomers 1, 2, and 3

To construct supramolecular BCPs under kinetic control, it is important to get detailed mechanistic insights into the pathway complexity and kinetics of supramolecular homopolymerization of individual monomers. Hence, kinetically controlled self-assembly of each monomer was probed by monitoring the absorbance and CD changes at 485 nm, 555 nm, and 360 nm for **1**, **2**, and **3**, respectively. The addition of monomeric **1** and **3** in TCE into TCE/MCH solvent mixture ([**1**] or [**3**] = 1.5×10^{-5} M, TCE/MCH, 10/90 (v/v)) resulted in the formation of a metastable state which transforms into supramolecular homopolymers, via a non-linear growth process with a lag phase (t_{lag} of 150 ± 12 seconds and 476 ± 5 seconds for **1** and **3**, respectively) (Figure 2b,d, S9, and S10) characteristic of a cooperative mechanistic pathway. On the other hand, monomers of **2** (TCE/MCH, 10/90 (v/v), [**2**] = 1.5×10^{-5} M) undergoes an instantaneous supramolecular homopolymerization. However, slow cooling ($-dT/dt$ = 1 K min^{-1}) of the monomers of **2** from 363 K, while probing the absorption changes at 555 nm revealed the presence of pathway complexity (Figure S11a,b) and monomers gets trapped in a high energy metastable state which over time gets transformed into the thermodynamically equilibrated homopolymeric state in a cooperative manner (Figure 2c, S11c). This suggests that the metastable state of the monomers of **2** can be accessed using fast cooling from high temperatures. The supramolecular polymerization kinetics of monomers **1**–**3**, obtained by the spectroscopic probing fits well with the Watzky-Finke autocatalytic model,[24] suggesting a nucleation-elongation pathway for the assembly process (Figure S9–S12). The presence of a cooperative supramolecular polymerization was further confirmed by temperature-dependent heating curves, which fits well with a cooperative nucleation elongation model (Figure S13). A decrease in lag time (t_{lag}) with an increase in concentration for monomers **1**–**3** assigned the metastable state as an on-pathway aggregates *en-route* to the thermodynamically stable supramolecular homopolymeric state.[5] In an attempt to investigate the nature of the metastable species we have recorded absorption, emission, CD and dynamic light scattering (DLS) spectra which indicated small ill-defined aggregates as the metastable state, prior to the nucleation and elongation event (Figure S14). However, detailed molecular-level characterization of the metastable aggregated state was hampered by its short lifetime. The observed pathway complexity and time-dependent nucleation-elongation growth mechanism are consistent with the use of diphenylalanine self-assembling peptide moiety, which is identified as one of the major components

responsible for amyloid fibril formation via a nucleation-elongation mechanism.[21] The crucial role of H-bonding between the peptide moiety in driving the self-assembly is evident from the FTIR studies in the solution phase (Figure S15).

Kinetically Controlled Two-Component Supramolecular Block Copolymers

Having established the kinetically controlled nucleation-growth supramolecular polymerization mechanism for the monomers **1**–**3**, we further attempted the synthesis of supramolecular BCPs via seeded LSP process by the sequential addition of monomers.[13] It has been shown recently that supramolecular BCPs can be synthesized under kinetic control by the introduction of seeds of one monomer to the metastable state of the other monomer, to trigger a hetero-seeding event. Following a similar strategy, we first targeted the synthesis of two-component supramolecular BCPs with different sequences such as $\mathbf{2}_{seed}$:$\mathbf{1}_{monomer}$, $\mathbf{3}_{seed}$:$\mathbf{2}_{monomer}$, and $\mathbf{3}_{seed}$:$\mathbf{1}_{monomer}$ in TCE/MCH solvent mixture (10/90 (v/v)). Seed solutions of **2** and **3** were prepared by the sonication of respective kinetically grown supramolecular homopolymers (10^{-4} M, TCE/MCH, 10/90, (v/v)) for 5 minutes (see the experimental section for details). Seed solutions were added to the metastable states of the required monomer and the time-dependent seeded growth was followed by monitoring the absorbance changes of the growing monomer (485 nm for **1** and 555 nm for **2**). The addition of $\mathbf{2}_{seed}$ to the metastable state of **1** ($[\mathbf{2}_{seed}]$:$[\mathbf{1}_{monomer}] = 0.6{:}1$, $[\mathbf{1}_{monomer}] = 1.5\times10^{-5}$ M) triggered an instantaneous growth of the monomers of **1** with faster rate compared to the independent homopolymerization of **1** (Figure 3a, S16, $t_{1/2} = 50$ seconds compared to $t_{1/2} =$ 386 seconds for unseeded assembly). Further, an increase in the concentration of $\mathbf{2}_{seed}$ leads to an accelerated transforma-

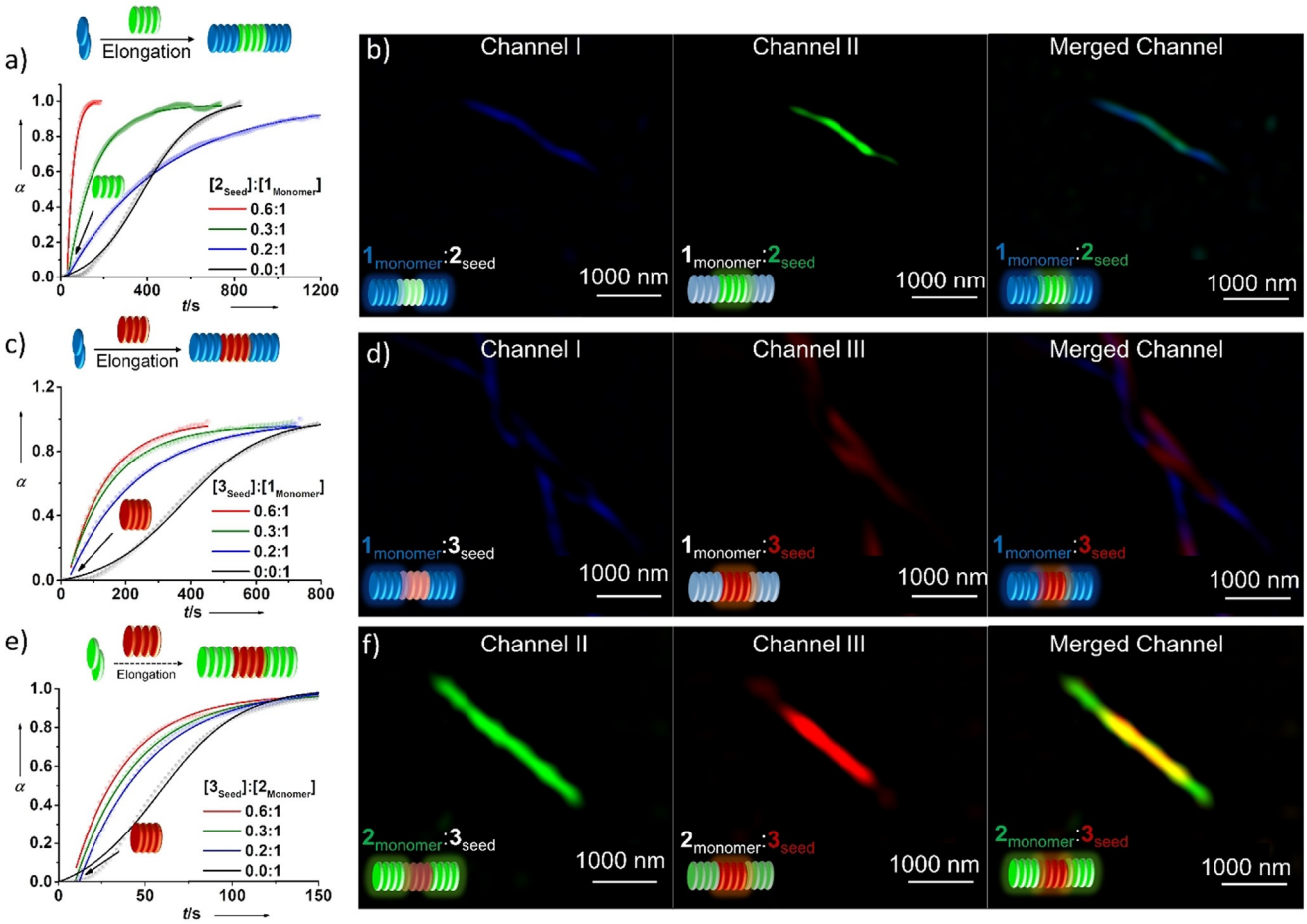

Figure 3. Time course of supramolecular polymerization on the addition of a) $\mathbf{2}_{seed}$ into the metastable state of **1** (monitored using absorbance changes at 485 nm) c) $\mathbf{3}_{seed}$ into the metastable state of **1** (monitored using absorbance changes at 485 nm) and e) $\mathbf{3}_{seed}$ into the metastable state of **2** (monitored using absorbance changes at 555 nm) ($[\mathbf{1}] = [\mathbf{2}] = [\mathbf{3}] = 1.5\times10^{-5}$ M, TCE/MCH, 10/90 (v/v)). The spontaneous growth of the monomers of **1** and **2**, without a lag phase, hints towards the heterogeneous seeding process. These experiments are performed for various monomer to seed ratios ([S]:[M]), which shows that the rate of growth of the second monomer decreases with a decrease in seed concentration, reiterating the seed-induced supramolecular polymerization process. SIM images of the synthesized two components supramolecular BCPs of b) $\mathbf{2}_{seed}$:$\mathbf{1}_{monomer}$ (0.6:1) imaged through channel I, and channel II, d) $\mathbf{3}_{seed}$:$\mathbf{1}_{monomer}$ (0.6:1) in channel I and channel III and f) $\mathbf{2}_{seed}$:$\mathbf{3}_{monomer}$ (0.6:1) in channel II and channel III, which shows the presence of connected green-blue, red-blue and yellow-blue segments, respectively (Channel I: $\lambda_{ex} = 488$ nm, $\lambda_{coll} = 495$–575; Channel II: $\lambda_{ex} = 561$ nm, $\lambda_{coll} = 570$–650, channel III: $\lambda_{ex} = 642$ nm, $\lambda_{coll} = 655$–800 nm).

tion of metastable **1** to its assembled state, characteristic of the heterogeneous seeded growth process (Figure 3a, S16).[25] Similar experimental results were obtained when **3** was used as a seed and **1** or **2** were used as monomers (($[\mathbf{3}_{seed}]$:$[\mathbf{1}_{monomer}] = 1{:}0.6$, $[\mathbf{1}] = 1.5\times10^{-5}$ M, and ($[\mathbf{3}_{seed}]$:$[\mathbf{2}_{monomer}] = 1{:}0.6$, $[\mathbf{2}] = 1.5\times10^{-5}$ M,) (Figure S17,S18). Absorption spectra of the resultant supramolecular copolymers show that individual aggregation characteristics of the monomers are retained, suggesting a segmented organization of the individual monomers (Figure S16d, S17d, S18d). All these observations corroborate to the formation of two-component supramolecular BCPs with $\mathbf{2}_{seed}$:$\mathbf{1}_{monomer}$, $\mathbf{3}_{seed}$:$\mathbf{1}_{monomer}$ and $\mathbf{3}_{seed}$:$\mathbf{2}_{monomer}$ composition. Further upon co-assembly, we have observed a significant quenching of donor emission (either monomer **1** or monomer **2**), which hints towards an energy transfer toward the acceptor molecules (**2** or **3**) with long-range exciton migration.[9] This further suggests the proximity between the self-assembled domains of two components, probably with a stacked organization leading to fast energy migration (Figure S16e, S17e, S18e, S19). However, the unequivocal proof for the supramolecular BCPs, is obtained from the detailed SIM imaging experiments, obtained by merging the Channel I, Channel II and Channel III (Figure 3b,d,f). In each supramolecular copolymer system, a mutually exclusive probing of the various monomeric components through different fluorescent channels facilitated the visualization of supramolecular BCPs. Although for supramolecular BCP between $\mathbf{2}_{seed}$:$\mathbf{1}_{monomer}$ and $\mathbf{3}_{seed}$:$\mathbf{2}_{monomer}$, $\mathbf{2}_{seed}$ and $\mathbf{3}_{seed}$ have an overlapped emission with $\mathbf{1}_{monomer}$ and $\mathbf{2}_{monomer,}$ respectively, the selective excitation and emission of the **1** and **2** monomers in one of the channels successfully aided the visualization process. Thus, supramolecular BCP of $\mathbf{2}_{seed}$:$\mathbf{1}_{monomer}$ shows connected segments of a green-emitting domain and blue-emitting domain with blue domain spanning over the entire fiber (due to overlapped emission of component **2** with component **1** in Channel I) (Figure 3b, S20). Likewise, the two-component block co-polymers between $\mathbf{3}_{seed}$:$\mathbf{1}_{monomer}$ and $\mathbf{3}_{seed}$:$\mathbf{2}_{monomer}$ depicted connected segments of red and blue-emitting domains (channel III and channel I) and connected segments of yellow (due to overlapped emission of component **3** and component **2** in channel II) and green-emitting domains (channel II and channel III), respectively (Figure 3e,f, S21, S22). We have further examined the kinetic stability and monomer exchange dynamics of the supramolecular block copolymers using time-dependent CD and absorption changes, which show unaltered spectral features over a period of 24 h (Figure S16f, S17f, and S18f). Further, time-dependent spectroscopic and SIM microscopic probing of a mixed seed solution of **2** and **3** homopolymers show narcissistically self-sorted supramolecular homopolymers, which remains stable over the period of 24 h (Figure S23). These observations reveal the low monomer exchange dynamics of the monomers and thus the high kinetic stability of these assemblies. Thus, although the SIM images portray a diffused interface between the connected segments, we can rule out any monomer diffusion between the blocky segments and ascribe the appearance of a diffused interface to the limited resolution of SIM ($\approx$120 nm). Further thermal annealing of the synthesized supramolecular BCPs results in the formation of random supramolecular copolymers (Figure S24). This suggests a comparable homo- and hetero- free energy of interaction between the monomers and hence the segmented organization could be achieved only by heterogeneous nucleation under kinetic control. Overall, the studies confirm an axial heterostructure topology between different fluorescent cNDI monomers formed by the supramolecular block polymerization under kinetic control.

Three-Component Supramolecular BCPs with Tunable Microstructure

The successful two-component seeded supramolecular block copolymerization of the monomers **1**–**3** and the resultant axial heterostructure morphology encouraged us to explore the next level of complexity of tricomponent supramolecular BCPs using sequential seeded supramolecular polymerization. Hence, we have first synthesized two-component green-red-green supramolecular BCP by the seeded growth of $\mathbf{2}_{monomer}$ with $\mathbf{3}_{seed}$ ($[\mathbf{2}_{monomer}]$:$[\mathbf{3}_{seed}] = 1{:}0.6$, $[\mathbf{2}_{monomer}] = 1.5\times10^{-5}$ M, TCE/MCH, 10/90 (v/v)) (Figure 4a, S25a,b). Next, to prepare the tricomponent BCP, we have utilized $\mathbf{3}_{seed}$:$\mathbf{2}_{monomer}$ BCP as the macro-seed, analogous to the macroinitiator in living radical covalent polymerization,[25] and monomers of **1** in TCE is introduced to the **2**:**3** BCP solution ($[\mathbf{3}_{seed}]$:$[\mathbf{2}_{monomer}]$:$[\mathbf{1}_{monomer}] = 0.6{:}1{:}1$, $[\mathbf{2}_{monomer}] = 1.5\times10^{-5}$ M, TCE/MCH, 10/90) and probed the time course of the growth of **1** using absorbance changes at 485 nm (Figure 4a, S25c). The addition of monomer **1**, in its metastable state into the $\mathbf{3}_{seed}$:$\mathbf{2}_{monomer}$ BCP macro-seed, induces an instant transformation of metastable **1** into the thermodynamically stable aggregates with a faster rate ($t_{1/2} = 36$ seconds in presence of diblock seed and $t_{1/2} = 354$ seconds in absence of seed) compared to the independent nucleation-elongation polymerization of **1**. This indicates that the incoming monomers of **1** nucleate and grow at the active ends of diblock co-polymer leading to a tri-component supramolecular block co-polymer with $\mathbf{3}_{seed}$:$\mathbf{2}_{monomer}$:$\mathbf{1}_{monomer}$ sequence. Absorption spectra of the tricomponent co-polymer retain the individual self-assembly characteristics of the constituent monomers, which implies the presence of segmented domains of **1**, **2**, and **3** (Figure S26). Finally, the fluorescent nature of the cNDI facilitated visualization of the tricomponent BCPs under SIM imaging (Figure 4b). The tricomponent supramolecular BCP polymer was visualized by merging channel I, channel II and channel III images, which showed characteristics of blue-green-red-green-blue emissive segmented topology, indicating a $\mathbf{3}_{seed}$:$\mathbf{2}_{monomer}$:$\mathbf{1}_{monomer}$ sequence in agreement with the sequential seeding process (Figure S27, S28, and S29). Thermal annealing of these tricomponent supramolecular BCPs again leads to the formation of a random supramolecular copolymer formation (Figure S30).

We have further investigated the possibility of synthesizing other tricomponent sequences by changing the order of addition of three monomers during the multi-step seeding process. Thus, we first prepared supramolecular diblock co-polymer seeds with $\mathbf{2}_{seed}$:$\mathbf{1}_{monomer}$ and $\mathbf{2}_{seed}$:$\mathbf{3}_{monomer}$ sequence by the addition of **1** and **3** monomers to the pre-synthesized seeds

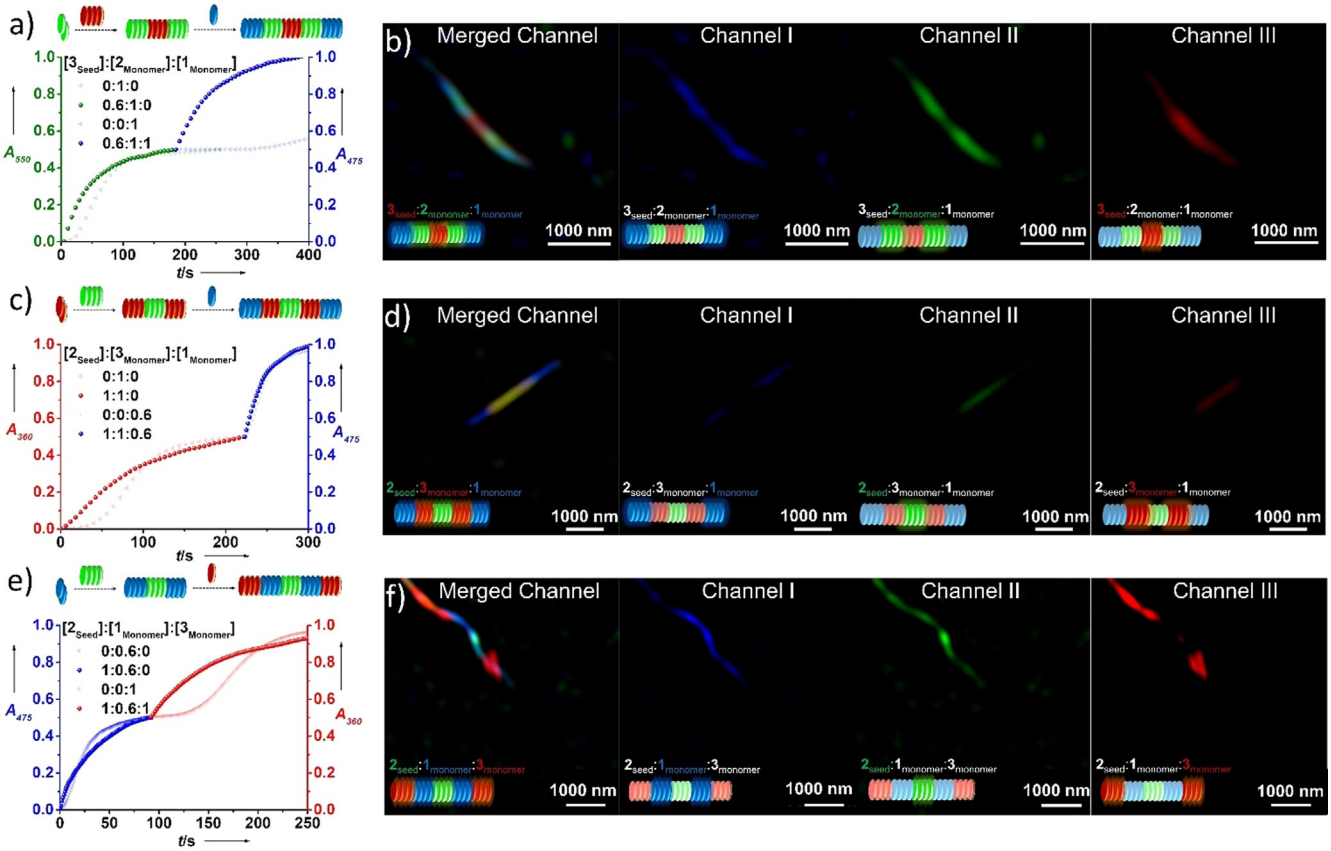

Figure 4. Synthesis of tricomponent supramolecular BCPs. Time course of supramolecular polymerization on sequential addition of a) $\mathbf{2}_{monomer}$ and $\mathbf{1}_{monomer}$ to $\mathbf{3}_{seed}$ (TCE/MCH, 10/90 (v/v), $[\mathbf{1}_{monomer}]=[\mathbf{2}_{monomer}]=1.5\times10^{-5}$ M], c) $\mathbf{3}_{monomer}$ and $\mathbf{1}_{monomer}$ to $\mathbf{2}_{seed}$ (TCE/MCH, 6/94 (v/v), $[\mathbf{3}_{monomer}]=2.5\times10^{-5}$ M, $[\mathbf{1}_{monomer}]=1.5\times10^{-5}$ M) and e) **1** monomer and **3** monomer to $\mathbf{2}_{seed}$ (TCE/MCH, 6/94 (v/v), $[\mathbf{1}_{monomer}]=1.5\times10^{-5}$ M, $[\mathbf{3}_{monomer}]=2.5\times10^{-5}$ M) to result in tricomponent supramolecular BCPs with sequences of $\mathbf{3}_{seed}$:$\mathbf{2}_{monomer}$:$\mathbf{1}_{monomer}$, $\mathbf{2}_{seed}$:$\mathbf{3}_{monomer}$:$\mathbf{1}_{monomer}$ and $\mathbf{2}_{seed}$:$\mathbf{1}_{monomer}$:$\mathbf{3}_{monomer}$, respectively. SIM images of b) $\mathbf{3}_{seed}$:$\mathbf{2}_{monomer}$:$\mathbf{1}_{monomer}$, d) $\mathbf{2}_{seed}$:$\mathbf{3}_{monomer}$:$\mathbf{1}_{monomer}$ and f) $\mathbf{2}_{seed}$:$\mathbf{1}_{monomer}$:$\mathbf{3}_{monomer}$ tricomponent block sequences in channel I, channel II, channel III and merged channel showing presence green-red-blue, red-green-blue, green-blue-red segments, respectively (Channel I: $\lambda_{ex}=488$ nm, $\lambda_{coll}=495$–575; Channel II: $\lambda_{ex}=561$ nm, $\lambda_{coll}=570$–650, channel III: $\lambda_{ex}=642$ nm, $\lambda_{coll}=655$–800 nm).

of **2** and the seeded growth could be probed by monitoring the absorbance changes at 485 nm and 360, respectively (Figure 4c,e, S31, S32). Next, to synthesize tricomponent supramolecular BCP of different sequences, we have introduced monomers of **1** to $\mathbf{2}_{seed}$:$\mathbf{3}_{monomer}$ diblock co-polymer seeds and monomers of **3** to $\mathbf{2}_{seed}$:$\mathbf{1}_{monomer}$ diblock co-polymer seeds (Figure 4c,e, S31c, S32c). Spectroscopic probing revealed the formation of tricomponent supramolecular BCPs with respect to faster kinetics of growth of the added monomers (Figure S31, S32). SIM imaging proved the presence of tricomponent supramolecular BCPs with characteristics of blue-red-green-red-blue and blue-red-green-red-blue emissive segmented topology is consistent with the expected $\mathbf{2}_{seed}$:$\mathbf{3}_{monomer}$:$\mathbf{1}_{monomer}$ and $\mathbf{2}_{seed}$:$\mathbf{1}_{monomer}$:$\mathbf{3}_{monomer}$ sequence (Figure 4d,f, S33–S37).

Conclusion

In conclusion, we have realized the synthesis of tricomponent supramolecular block copolymers of cNDI π-conjugated monomers via a sequential seeded supramolecular polymerization process. Diphenylalanine appended, structurally similar cNDI monomers with different core-substitution used in the present study exhibited a kinetically controlled cooperative supramolecular polymerization through an on-pathway metastable state. Utilizing the pathway complexity exhibited by these monomers, first, we have synthesized two-component supramolecular BCPs with different sequences by the kinetically controlled, seeded supramolecular polymerization process with supramolecular homopolymers as seeds and metastable states of **1**–**3** as monomer feeds. We have further used the two-component supramolecular BCPs as the macro-seeds for the synthesis of tri-component BCPs by the subsequent addition of different metastable monomers. Thus, tricomponent supramolecular BCPs with different sequences could be synthesized by varying the order of monomer addition during the sequential seeded supramolecular polymerization process. The distinct spectral properties of the various cNDI chromophores, which are used as the monomers here, facilitated the in situ selective spectroscopic probings of the heterogenous seeding process during the sequential seeding process with different derivatives. Further distinct blue, green, and red fluorescent nature of the three cNDI monomers, aided the characterization of the different microstructure of the resultant multi-component self-assembled

nanostructures with super-resolved structured illumination microscopy imaging.

The unprecedented synthesis of tricomponent supramolecular BCPs via sequential seeded supramolecular polymerization demonstrated here is analogous to the use of macroinitiators in the free-radical living polymerization synthesis of covalent block copolymers. We envisage that the results presented here provide a significant advancement in the synthesis of complex supramolecular BCPs with tunable microstructure. Further, the resultant axial heterostructure topology with multiple organic semi-conducting monomers provides unique opportunities for light harvesting, energy migration and catalysis, which will be investigated in near future.

Acknowledgements

We would also like to thank JNCASR and the Department of Science and Technology, Government of India, for financial support. In addition, the funding from Sheikh Saqr Laboratory (SSL), JNCASR is also acknowledged. S. J. G. acknowledges the funding received from SwarnaJayanti Fellowship Award (DST/SJF/CSA01/2016–2017) and Department of Biotechnology, Government of India, for the Indo-Switzerland Joint Research project (BT/IN/Swiss/55/SJG/2018–2019). S.S.A acknowledges support from DST-SERB CRG Grant (CRG/2020/006183). AS, RS and AD thank CSIR for fellowships.

Conflict of Interest

The authors declare no conflict of interest.

Keywords: peptide · seeded growth · self-assembly · supramolecular block copolymers · supramolecular polymers

[1] a) T. Aida, E. W. Meijer, S. I. Stupp, *Science* **2012**, *335*, 813 – 817; b) A. Jain, S. J. George, *Mater. Today* **2015**, *18*, 206 – 214; c) G. Vantomme, E. W. Meijer, *Science* **2019**, *363*, 1396 – 1397; d) T. Aida, E. W. Meijer, *Isr. J. Chem.* **2020**, *60*, 33 – 47; e) P. K. Hashim, J. Bergueiro, E. W. Meijer, T. Aida, *Prog. Polym. Sci.* **2020**, *105*, 101250.

[2] a) P. Jonkheijm, P. van der Schoot, A. P. H. J. Schenning, E. W. Meijer, *Science* **2006**, *313*, 80 – 83; b) T. F. A. De Greef, M. M. J. Smulders, M. Wolffs, A. P. H. J. Schenning, R. P. Sijbesma, E. W. Meijer, *Chem. Rev.* **2009**, *109*, 5687 – 5754; c) M. M. J. Smulders, M. M. L. Nieuwenhuizen, T. F. A. de Greef, P. van der Schoot, A. P. H. J. Schenning, E. W. Meijer, *Chem. Eur. J.* **2010**, *16*, 362 – 367; d) C. Kulkarni, S. Balasubramanian, S. J. George, *ChemPhysChem* **2013**, *14*, 661 – 673.

[3] a) P. A. Korevaar, S. J. George, A. J. Markvoort, M. M. Smulders, P. A. Hilbers, A. P. H. J. Schenning, T. F. A. de Greef, E. W. Meijer, *Nature* **2012**, *481*, 492 – 496; b) P. A. Korevaar, T. F. A. de Greef, E. W. Meijer, *Chem. Mater.* **2014**, *26*, 576 – 586; c) A. Sorrenti, J. L. Iglesias, A. J. Markvoort, T. F. A. de Greef, T. M. Hermans, *Chem. Soc. Rev.* **2017**, *46*, 5476 – 5490; d) A. Langenstroer, K. K. Kartha, Y. Dorca, J. Droste, V. Stepanenko, R. Q. Albuquerque, M. R. Hansen, L. Sanchez, G. Fernandez, *J. Am. Chem. Soc.* **2019**, *141*, 5192 – 5200; e) E. E. Greciano, J. Calbo, E. Ortí, L. Sánchez, *Angew. Chem. Int. Ed.* **2020**, *59*, 17517 – 17524; *Angew. Chem.* **2020**, *132*, 17670 – 17677; f) M. Wehner, M. I. S. Röhr, V. Stepanenko, F. Würthner, *Nat. Commun.* **2020**, *11*, 5460; g) T. Schnitzer, G. Vantomme, *ACS Cent. Sci.* **2020**, *6*, 2060 – 2070; h) H. Choi, S. Heo, S. Lee, K. Y. Kim, J. H. Lim, S. H. Jung, S. S. Lee, H. Miyake, J. Y. Lee, J. H. Jung, *Chem. Sci.* **2020**, *11*, 721 – 730.

[4] a) D. van der Zwaag, T. F. A. De Greef, E. W. Meijer, *Angew. Chem. Int. Ed.* **2015**, *54*, 8334 – 8336; *Angew. Chem.* **2015**, *127*, 8452 – 8454; b) R. D. Mukhopadhyay, A. Ajayaghosh, *Science* **2015**, *349*, 241; c) J. Matern, Y. Dorca, L. Sànchez, G. Fernàndez, *Angew. Chem. Int. Ed.* **2019**, *58*, 16730 – 16740; *Angew. Chem.* **2019**, *131*, 16884 – 16895.

[5] a) S. Ogi, K. Sugiyasu, S. Manna, S. Samitsu, M. Takeuchi, *Nat. Chem.* **2014**, *6*, 188 – 195; b) J. Kang, D. Miyajima, T. Mori, Y. Inoue, Y. Itoh, T. Aida, *Science* **2015**, *347*, 646 – 651; c) S. Ogi, V. Stepanenko, K. Sugiyasu, M. Takeuchi, F. Würthner, *J. Am. Chem. Soc.* **2015**, *137*, 3300 – 3307; d) S. Ogi, V. Stepanenko, J. Thein, F. Würthner, *J. Am. Chem. Soc.* **2016**, *138*, 670 – 678; e) T. Fukui, S. Kawai, S. Fujinuma, Y. Matsushita, T. Yasuda, T. Sakurai, S. Seki, M. Takeuchi, K. Sugiyasu, *Nat. Chem.* **2017**, *9*, 493 – 499; f) B. Kemper, L. Zengerling, D. Spitzer, R. Otter, T. Bauer, P. Besenius, *J. Am. Chem. Soc.* **2018**, *140*, 534 – 537; g) S. Ogi, K. Matsumoto, S. Yamaguchi, *Angew. Chem. Int. Ed.* **2018**, *57*, 2339 – 2343; *Angew. Chem.* **2018**, *130*, 2363 – 2367; h) E. E. Greciano, B. Matarranz, L. Sanchez, *Angew. Chem. Int. Ed.* **2018**, *57*, 4697 – 4701; *Angew. Chem.* **2018**, *130*, 4787 – 4791; i) T. Fukui, N. Sasaki, M. Takeuchi, K. Sugiyasu, *Chem. Sci.* **2019**, *10*, 6770 – 6776; j) S. Sarkar, A. Sarkar, S. J. George, *Angew. Chem. Int. Ed.* **2020**, *59*, 19841 – 19845; *Angew. Chem.* **2020**, *132*, 20013 – 20017; k) H. Choi, S. Ogi, N. Ando, S. Yamaguchi, *J. Am. Chem. Soc.* **2021**, *143*, 2953 – 2961; l) I. Helmers, G. Ghosh, R. Q. Albuquerque, G. Fernández, *Angew. Chem. Int. Ed.* **2021**, *60*, 4368 – 4376; *Angew. Chem.* **2021**, *133*, 4414 – 4423; m) G. Moreno-Alcàntar, A. Aliprandi, R. Rouquette, L. Pesce, K. Wurst, C. Perego, P. Brgggeller, G. M. Pavan, L. D. Cola, *Angew. Chem. Int. Ed.* **2021**, *60*, 5407 – 5413; *Angew. Chem.* **2021**, *133*, 5467 – 5473; n) V. Faramarzi, F. Niess, E. Moulin, M. Maaloum, J. Dayen, J. Beaufrand, S. Zanettini, B. Doudin, N. Giuseppone, *Nat. Chem.* **2012**, *4*, 485 – 490; o) T. K. Ellis, M. Galerne, J. J. Armao, A. Osypenko, D. Martel, M. Maaloum, G. Fuks, O. Gavat, E. Moulin, N. Giuseppone, *Angew. Chem. Int. Ed.* **2018**, *57*, 15749 – 15753; *Angew. Chem.* **2018**, *130*, 15975 – 15979; p) A. Aliprandi, M. Mauro, L. D. Cola, *Nat. Chem.* **2016**, *8*, 10 – 15; q) M. E. Robinson, D. J. Lunn, A. Nazemi, G. R. Whittell, L. D. Cola, I. Manners, *Chem. Commun.* **2015**, *51*, 15921 – 15924.

[6] a) X. Wang, G. Guerin, H. Wang, Y. Wang, I. Manners, M. Winnik, *Science* **2007**, *317*, 644 – 648; b) T. Gädt, N. S. Ieong, G. Cambridge, M. A. Winnik, I. Manners, *Nat. Mater.* **2009**, *8*, 144 – 150; c) J. B. Gilroy, T. Gadt, G. R. Whittell, L. Chabanne, J. M. Mitchels, R. M. Richardson, M. A. Winnik, I. Manners, *Nat. Chem.* **2010**, *2*, 566 – 570; d) Z. M. Hudson, C. E. Boott, M. E. Robinson, P. A. Rupar, M. A. Winnik, I. Manners, *Nat. Chem.* **2014**, *6*, 893 – 898.

[7] a) M. Endo, T. Fukui, S. H. Jung, S. Yagai, M. Takeuchi, K. Sugiyasu, *J. Am. Chem. Soc.* **2016**, *138*, 14347 – 14353; b) S. Dhiman, S. J. George, *Bull. Chem. Soc. Jpn.* **2018**, *91*, 687 – 699; c) S. Dhiman, A. Sarkar, S. J. George, *RSC Adv.* **2018**, *8*, 18913 – 18925; d) A. Mishra, D. B. Korlepara, M. Kumar, A. Jain, N. Jonnalagadda, K. K. Bejagam, S. Balasubramanian, S. J. George, *Nat. Commun.* **2018**, *9*, 1295; e) A. Jain, S. Dhiman, A. Dhayani, P. K. Vemula, S. J. George, *Nat. Commun.* **2019**, *10*, 450; f) K. Jalani, A. Devi Das, R. Sasmal, S. S. Agasti, S. J. George, *Nat. Commun.* **2020**, *11*, 3967; g) S. Dhiman, R. Ghosh, S. Sarkar, S. J. George, *Chem. Sci.* **2020**, *11*, 12701 – 12709; h) A. Mishra, S. Dhiman, S. J. George, *Angew. Chem. Int. Ed.* **2021**, *60*, 2740 – 2756; *Angew. Chem.* **2021**, *133*, 2772 – 2788.

[8] a) P. Besenius, *Polym. Chem.* **2017**, *55*, 34 – 78; b) B. Adelizzi, N. J. Van Zee, L. N. De Windt, A. R. Palmans, E. W. Meijer, *J. Am. Chem. Soc.* **2019**, *141*, 6110 – 6121; c) M. Wehner, F. Würthner, *Nat. Rev. Chem.* **2020**, *4*, 38 – 53; d) E. Weyandt, M. F. J. Mabesoone, L. N. J. de Windt, E. W. Meijer, A. R. A. Palmans, G. Vantomme, *Org. Mater.* **2020**, *2*, 129 – 142; e) L. MacFarlane, C. Zhao, J. Cai, H. Qiu, I. Manners, *Chem. Sci.* **2021**, *12*, 4661 – 4682.

[9] a) A. T. Haedler, K. Kreger, A. Issac, B. Wittmann, M. Kivala, N. Hammer, J. Köhler, H.-W. Schmidt, R. Hildner, *Nature* **2015**, *523*, 196 – 200; b) B. Wittmann, F. A. Wenzel, S. Wiesneth, A. T. Haedler, M. Drechsler, K. Kreger, J. Köhler, E. W. Meijer, H. W. Schmidt, R. Hildner, *J. Am. Chem. Soc.* **2020**, *142*, 8323 – 8330.

[10] a) Y. Yamamoto, T. Fukushima, Y. Suna, N. Ishii, A. Saeki, S. Seki, S. Tagawa, M. Taniguchi, T. Kawai, T. Aida, *Science* **2006**, *314*, 1761 – 1763; b) A. S. Weingarten, R. V. Kazantsev, L. C. Palmer, M. McClendon, A. R. Koltonow, A. P. S. Samuel, D. J. Kiebala, M. R. Wasielewski, S. I. Stupp, *Nat. Chem.* **2014**, *6*, 964 – 970; c) J. Tian, Y. Zhang, L. Du, Y. He, X. Jin, S. Pearce, J. C. Eloi, R. L. Harniman, D. Alibhai, R. Ye, D. L. Phillips, I. Manners, *Nat. Chem.* **2020**, *12*, 1150 – 1156.

[11] a) K. A. Davis, K. Matyjaszewski, *Adv. Polym. Sci.* **2002**, *159*, 1 – 166; b) H. Gao, K. Matyjaszewski, *Prog. Polym. Sci.* **2009**, *34*, 317 – 350.

[12] a) B. Adelizzi, A. Aloi, A. J. Markvoort, H. M. M. ten Eikelder, I. K. Voets, A. R. A. Palmans, E. W. Meijer, *J. Am. Chem. Soc.* **2018**, *140*, 7168 – 7175; b) A. Sarkar, T. Behera, R. Sasmal, R. Capelli, C. Empereur-mot, J. Mahato, S. S. Agasti, G. M. Pavan, A. Chowdhury, S. J. George, *J. Am. Chem. Soc.* **2020**, *142*, 11528 – 11539; c) B. Adelizzi, P. Chidchob, N. Tanaka, B. A. G. Lamers, S. C. J. Meskers, S. Ogi, A. R. A. Palmans, S. Yamaguchi, E. W. Meijer, *J. Am. Chem. Soc.* **2020**, *142*, 16681 – 16689.

[13] a) A. Pal, M. Malakoutikhah, G. Leonetti, M. Tezcan, M. Colomb-Delsuc, V. Nguyen, J. van der Gucht, S. Otto, *Angew. Chem. Int. Ed.* **2015**, *54*, 7852 – 7856; *Angew. Chem.* **2015**, *127*, 7963 – 7967; b) W. Wagner, M. Wehner, V. Stepanenko, F. Würthner, *J. Am. Chem. Soc.* **2019**, *141*, 12044 – 12054; c) W. Wagner, M. Wehner, V. Stepanenko, F. Würthner, *CCS Chem.* **2019**, *1*, 598 – 613; d) A. Sarkar, R. Sasmal, C. Empereur-mot, D. Bochicchio, S. V. K. Kompella, K. Sharma, S. Dhiman, B. Sundaram, S. S. Agasti, G. M. Pavan, S. J. George, *J. Am. Chem. Soc.* **2020**, *142*, 7606 – 7617; e) Q. Wan, W. To, X. Chang, C.-M. Che, *Chem* **2020**, *6*, 1 – 23; f) A. Sarkar, R. Sasmal, A. Das, S. S. Agasti, S. J. George, *Chem. Commun.* **2021**, *57*, 3937 – 3940.

[14] a) W. Zhang, W. Jin, T. Fukushima, A. Saeki, S. Seki, T. Aida, *Science* **2011**, *334*, 340 – 343; b) W. Zhang, W. Jin, T. Fukushima, T. Mori, T. Aida, *J. Am. Chem. Soc.* **2015**, *137*, 13792 – 13795; c) S. H. Jung, D. Bochicchio, G. M. Pavan, M. Takeuchi, K. Sugiyasu, *J. Am. Chem. Soc.* **2018**, *140*, 10570 – 10577; d) N. Sasaki, M. F. J. Mabesoone, J. Kikkawa, T. Fukui, N. Shioya, T. Shimoaka, T. Hasegawa, H. Takagi, R. Haruki, N. Shimizu, S. Adachi, E. W. Meijer, M. Takeuchi, K. Sugiyasu, *Nat. Commun.* **2020**, *11*, 3578; e) S. Datta, Y. Kato, S. Higashiharaguchi, K. Aratsu, A. Isobe, T. Saito, D. D. Prabhu, Y. Kitamoto, M. J. Hollamby, A. J. Smith, R. Dagleish, N. Mahmoudi, L. Pesce, C. Perego, G. M. Pavan, S. Yagai, *Nature* **2020**, *583*, 400 – 405.

[15] a) F. S. Bates, M. A. Hillmyer, T. P. Lodge, C. M. Bates, K. T. Delaney, G. H. Fredrickson, *Science* **2012**, *336*, 434 – 440; b) P. B. Zetterlund, S. C. Thickett, S. Perrier, E. Bourgeat-Lami, M. Lansalot, *Chem. Rev.* **2015**, *115*, 9745 – 9800.

[16] J. M. Hudson, D. J. Lunn, M. A. Winnik, I. Manners, *Nat. Commun.* **2014**, *5*, 3372.

[17] a) M. M. Safont-Sempere, G. Fernandez, F. Würthner, *Chem. Rev.* **2011**, *111*, 5784 – 5814; b) K. L. Morris, L. Chen, J. Raeburn, O. R. Sellick, P. Cotanda, A. Paul, P. C. Griffiths, S. M. King, R. K. O'Reilly, L. C. Serpell, D. J. Adams, *Nat. Commun.* **2013**, *4*, 1480; c) S. Prasanthkumar, S. Ghosh, V. C. Nair, A. Saeki, S. Seki, A. Ajayaghosh, *Angew. Chem. Int. Ed.* **2015**, *54*, 946 – 950; *Angew. Chem.* **2015**, *127*, 960 – 964; d) E. R. Draper, E. G. B. Eden, T. O. McDonald, D. J. Adams, *Nat. Chem.* **2015**, *7*, 848 – 852; e) D. J. Cornwell, O. J. Daubney, D. K. Smith, *J. Am. Chem. Soc.* **2015**, *137*, 15486 – 15492; f) B. Narayan, K. K. Bejagam, S. Balasubramanian, S. J. George, *Angew. Chem. Int. Ed.* **2015**, *54*, 13053 – 13057; *Angew. Chem.* **2015**, *127*, 13245 – 13249; g) S. Onogi, H. Shigemitsu, T. Yoshii, T. Tanida, M. Ikeda, R. Kubota, I. Hamachi, *Nat. Chem.* **2016**, *8*, 743 – 752; h) A. Sandeep, V. K. Praveen, K. K. Kartha, V. Karunakaran, A. Ajayaghosh, *Chem. Sci.* **2016**, *7*, 4460; i) A. Sarkar, S. Dhiman, A. Chalishazar, S. J. George, *Angew. Chem. Int. Ed.* **2017**, *56*, 13767 – 13771; *Angew. Chem.* **2017**, *129*, 13955 – 13959; j) H. Shigemitsu, T. Fujisaku, W. Tanaka, R. Kubota, S. Minami, K. Urayama, I. Hamachi, *Nat. Nanotechnol.* **2018**, *13*, 165 – 172.

[18] a) F. Würthner, S. Ahmed, C. Thalacker, T. Debaerdemaeker, *Chem. Eur. J.* **2002**, *8*, 4742 – 4750; b) N. Sakai, J. Mareda, E. Vauthey, S. Matile, *Chem. Commun.* **2010**, *46*, 4225 – 4237; c) A. Nowak-Król, K. Shoyama, M. Stolte, F. Würthner, *Chem. Commun.* **2018**, *54*, 13763 – 13772.

[19] a) G. Sforazzini, E. Orentas, A. Bolag, N. Sakai, S. Matile, *J. Am. Chem. Soc.* **2013**, *135*, 12082 – 12090; b) P. Charbonnaz, Y. Zhao, R. Turdean, S. Lascano, N. Sakai, S. Matile, *Chem. Eur. J.* **2014**, *20*, 17143.

[20] a) A. L. Sisson, N. Sakai, N. Banerji, A. Fürstenberg, E. Vauthey, S. Matile, *Angew. Chem. Int. Ed.* **2008**, *47*, 3727 – 3729; *Angew. Chem.* **2008**, *120*, 3787 – 3789; b) N. Sakai, R. Bhosale, D. Emery, J. Mareda, S. Matile, *J. Am. Chem. Soc.* **2010**, *132*, 6923 – 6925.

[21] a) P. Arosio, T. P. J. Knowles, S. Linse, *Phys. Chem. Chem. Phys.* **2015**, *17*, 7606 – 7618; b) D. Boyd-Kimball, H. M. Abdul, T. Reed, R. Sultana, D. A. Butterfield, *Chem. Res. Toxicol.* **2004**, *17*, 1743 – 1749.

[22] a) H. Shao, T. Nguyen, N. C. Romano, D. A. Modarelli, J. R. Parquette, *J. Am. Chem. Soc.* **2009**, *131*, 16374 – 16376; b) S. Tu, S. H. Kim, J. Joseph, D. A. Modarelli, J. R. Parquette, *J. Am. Chem. Soc.* **2011**, *133*, 19125 – 19130; c) S. Fleming, R. V. Ulijn, *Chem. Soc. Rev.* **2014**, *43*, 8150 – 8177; d) S. K. M. Nalluri, C. Berdugo, N. Javid, P. W. J. M. Frederix, R. V. Ulijn, *Angew. Chem. Int. Ed.* **2014**, *53*, 5882 – 5887; *Angew. Chem.* **2014**, *126*, 5992 – 5997; e) A. M. Sanders, T. J. Magnanelli, A. E. Bragg, J. D. Tovar, *J. Am. Chem. Soc.* **2016**, *138*, 3362 – 3370; f) N. Singha, P. Gupta, B. Pramanik, S. Ahmed, A. Dasgupta, A. Ukil, D. Das, *Biomacromolecules* **2017**, *18*, 3630 – 3641; g) M. Kumar, N. L. Ing, V. Narang, N. K. Wijerathne, A. I. Hochbaum, R. V. Ulijn, *Nat. Chem.* **2018**, *10*, 696 – 703; h) M. B. Avinash, T. Govindaraju, *Acc. Chem. Res.* **2018**, *51*, 414 – 426; i) A. Sarkar, J. C. Kölsch, C. M. Berač, A. Venugopal, R. Sasmal, R. Otter, P. Besenius, S. J. George, *ChemistryOpen* **2020**, *9*, 346 – 350.

[23] a) S. Pujals, N. Feiner-Gracia, P. Delcanale, I. Voets, L. Albertazzi, *Nat. Rev. Chem.* **2019**, *3*, 68 – 84; b) R. Kubota, K. Nakamura, S. Torigoe, I. Hamachi, *ChemistryOpen* **2020**, *9*, 67 – 79.

[24] L. Bentea, M. A. Watzky, R. G. Finke, *J. Phys. Chem. C* **2017**, *121*, 5302 – 5312.

[25] G. G. Odian, *Principle of Polymerization*, 3rd ed., Wiley, Hoboken, **1991**.

Manuscript received: April 19, 2021
Revised manuscript received: May 25, 2021
Accepted manuscript online: June 10, 2021
Version of record online: July 5, 2021

